Geophysical Journal International

Geophys. J. Int. (2017) **210,** 534–548
Advance Access publication 2017 May 8
GJI Marine geosciences and applied geophysics

doi: 10.1093/gji/ggx194

Directional structure tensors in estimating seismic structural and stratigraphic orientations

Xinming Wu and Xavier Janson

*Bureau of Economic Geology, The University of Texas at Austin, Austin, TX*78758, *USA. E-mail: xinming.wu@beg.utexas.edu*

Accepted 2017 May 5. Received 2017 May 3; in original form 2017 January 4

SUMMARY

Estimating orientations of seismic structures (reflections) and stratigraphic features (channels) is important for seismic interpretation, subsurface interpolation and geophysical inversion. Structure tensors, constructed as smoothed outer products of amplitude gradients, are commonly used to estimate seismic reflection normals, which uniquely define the reflection orientations. However, this conventional structure-tensor method often generates significant errors in estimating orientations of the reflections with steep and rapidly varying slopes. To better estimate reflection orientations, we propose to construct structure tensors in a new space, where the reflections are mostly flat or only slightly dipping and the variation of reflection slopes is reduced. We use these constructed structure tensors to compute reflection normals in this new space and then transform the normals back to obtain a better estimation of reflection orientations in the original space. Seismic stratigraphic features such as channels are often aligned within dipping reflections. It is not discussed previously by others to estimate orientations of such features directly from a seismic image. An ideal way to estimate stratigraphic orientations is to first extract a horizon surface with stratigraphic features, and then construct structure tensors with gradients on the surface to estimate the orientations of the features. However, extracting horizon surfaces can be a difficult and time-consuming task in practice. Fortunately, computing gradients on a horizon surface is only a local operation and is equivalent to directly compute directional derivatives along reflection slopes without picking horizons. Based on this observation, we propose to use an equivalent but more efficient way to estimate seismic stratigraphic orientations by using structure tensors constructed with the directional derivatives along reflections. We demonstrate the methods of estimating structural and stratigraphic orientations using 3-D synthetic and real examples.

Key words: Image processing; Numerical solutions; Inverse theory; Numerical approximations and analysis.

1 INTRODUCTION

A seismic image contains useful structural and stratigraphic features such as reflections and channels. Reflections are the dominant features in a seismic image while the stratigraphic features are aligned within the dipping reflections. Estimating the orientations of the seismic structural and stratigraphic features is helpful to enhance such features (e.g. Bakker 2002; Fehmers & Höcker 2003; Hale 2009b), to interpret horizons (e.g. Lomask *et al.* 2006; Parks 2010; Fomel 2010; Luo & Hale 2013; Wu & Hale 2015b) and to incorporate the structural and stratigraphic constraints in subsurface modelling (Hale 2009a; Wu 2017a) and geophysical inversion (Li & Oldenburg 2000; Clapp *et al.* 2004; Ma *et al.* 2012; Wu 2017b).

As discussed by Marfurt (2006), the local reflection orientation can be described by reflection normal vector, or by inline and crossline slopes, or equivalently by dip and azimuth. To estimate reflection orientations, Bakker (2002) and Wu & Hale (2015a) use structure tensors (e.g. Van Vliet & Verbeek 1995; Weickert 1997) to compute reflection normal vectors. Fomel (2002) and Arias (2016) use plane-wave destruction (Claerbout 1992) and dynamic image warping (Hale 2013), respectively, to compute the inline and crossline reflection slopes. Marfurt (2006) and Yu *et al.* (2013) compute the reflection dip and azimuth by coherence scanning and using 2-D Log-Gabor filter (Field 1987), respectively. Although numerous methods have been proposed to estimate seismic reflection orientations. It is still a challenge to estimate the orientations of reflections with steep and rapidly varying slopes. In addition, estimating seismic stratigraphic orientations is not discussed in these methods. In this paper, we propose methods to more accurately estimate seismic structural and stratigraphic orientations by using directional structure tensors.

As the conventional structure-tensor method often generates errors in estimating orientations of reflections with steep and rapidly varying slopes, we propose to estimate reflection orientations in a new space, where the reflections are all flat or only slightly dipping and the reflection slopes spatially vary slowly. To define such a space, we first use the conventional structure tensors to compute an initial estimation of the reflection normal vectors **u**, from which we compute the other two orthogonal vectors **p** and **q** that are orthogonal to **u** and approximately aligned within reflections. With the three orthogonal vectors, we define a new *upq* space, which is similar to the *uvt* space discussed by Mallet (2004, 2014), the stratigraphic space discussed by Karimi & Fomel (2015), and the rotated space discussed by Di & Gao (2016). In such a space, seismic reflections are almost flat or only slightly dipping in areas where the initial reflection normals **u** are not accurate enough.

To estimate the reflection orientation in the new *upq* space, we do not need to explicitly transform the original seismic image into this new space. Constructing structure tensors in the new space requires only the image gradients in that space. It is a local operation to compute the gradients in the new space, which is equivalent to compute directional derivatives in directions along the vectors **u**, **p** and **q**. Therefore, we can efficiently construct structure tensors in the new space with the directional derivatives to estimate the reflection normals in the new space. We then use a transformation matrix defined by vectors **u**, **p** and **q** to transform these normal vectors back to obtain an accurate estimation of the reflection normals in the original space.

To compute orientations of stratigraphic features that are aligned within reflections, we only need to estimate how the stratigraphic features are laterally oriented along seismic reflections because we have already estimated the reflection normals. To estimate the lateral orientations of the stratigraphic features, we can also construct directional structure tensors but with only the directional derivatives along vectors **p** and **q** that are aligned within reflections. Combining with the estimated lateral stratigraphic orientations and the reflection normals (that are also perpendicular to stratigraphic features), we are able to describe how the stratigraphic features are oriented in 3-D space. To demonstrate the methods of directional structure tensors in estimating structural and stratigraphic features, we applied the methods to both synthetic and real 3-D examples and compared the results with those computed from the conventional structure tensors.

2 CONVENTIONAL STRUCTURE TENSORS

To demonstrate the methods of estimating structural and stratigraphic orientations, we created a 3-D synthetic example with an unconformity, a fault, folded layers, and a channel as shown in Figs 1 and 2. In creating this synthetic example, we first define a simple reflectivity model with all flat layers, in which a sinusoidal shape channel is defined with relatively high reflectivities. We then vertically sheared the flat model to create folding and dipping structures. Next, we added several flat layers on the top to create an unconformity between these flat layers above and the folded layers below. We finally added a planar fault by sliding model blocks on opposite sides of the fault with some specific vector shifts. With the folded and faulted reflectivity model, we compute the seismic image shown in Figs 1(a) and 2(a) by convolving the reflectivity model with a Ricker wavelet in directions perpendicular to the structures, and adding some random noise with RMS = 0.5. Figs 1(b) and (c),

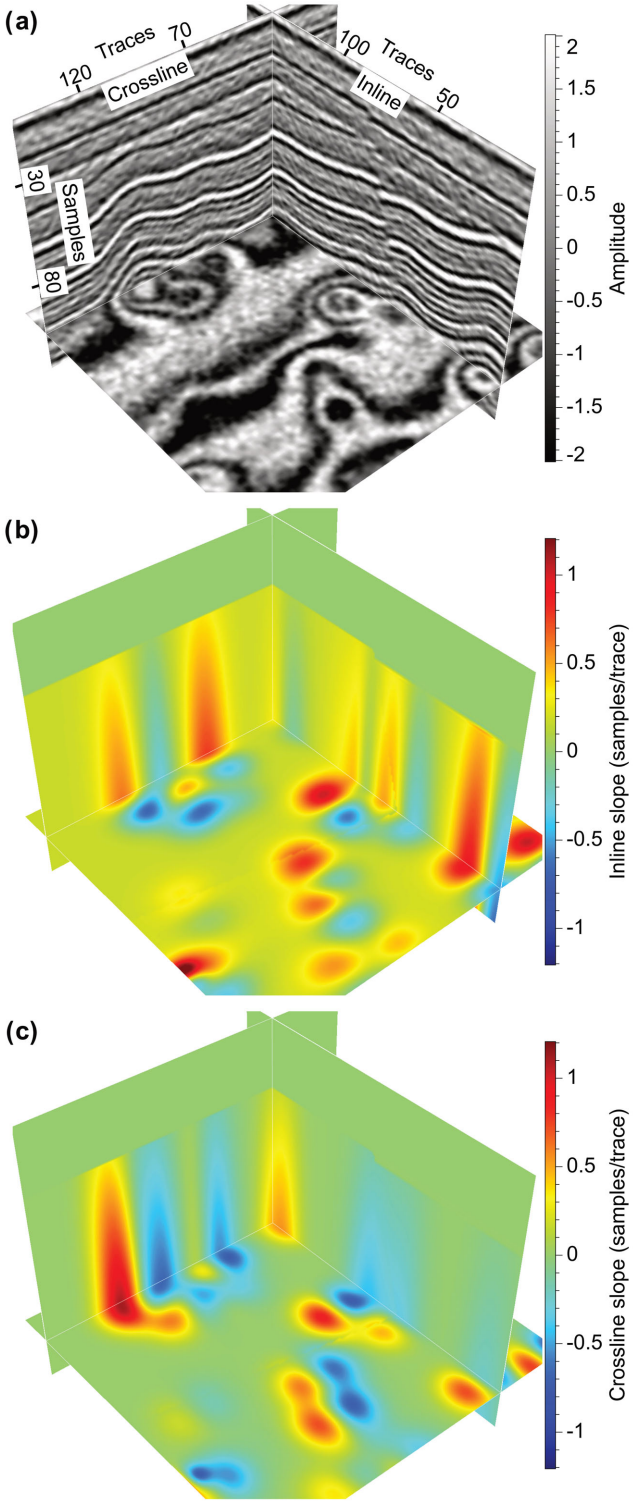

Figure 1. A noisy synthetic seismic image (a) and corresponding true inline (b) and crossline (c) slopes.

respectively, show the true inline and crossline reflection slopes that we used to create the folding and dipping in the reflectivity model. The horizon surface in Fig. 2(a) displays a sinusoidal channel. We describe the orientation of the channel using the azimuth α as defined in Fig. 2(a), and the true azimuth of the channel is displayed in colours on the channel in Fig. 2(b).

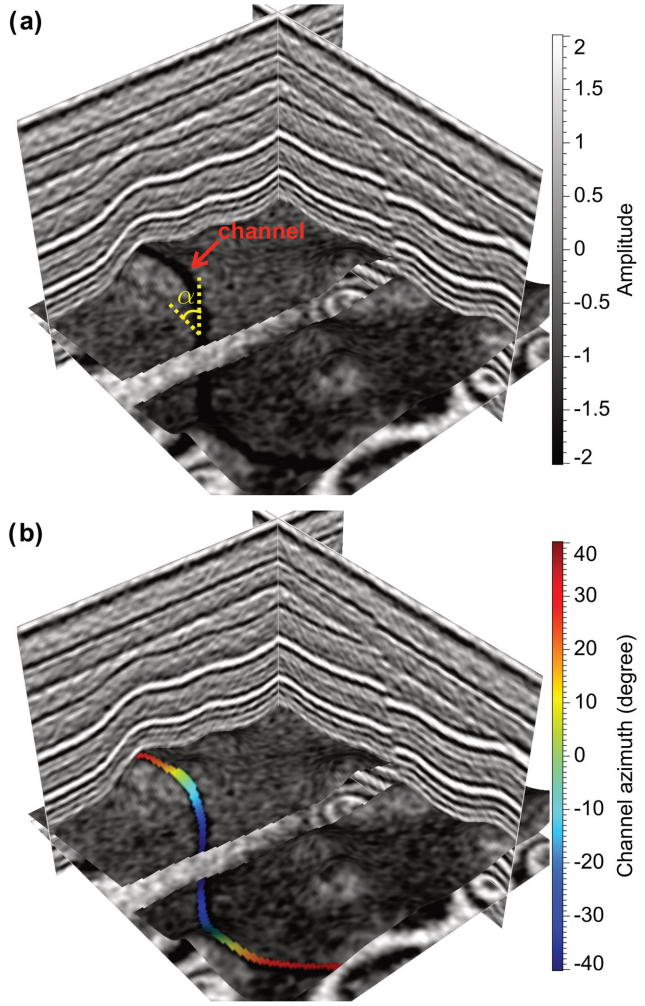

Figure 2. The seismic image is displayed with a channel (a) and the azimuth (b) of the channel on a seismic horizon surface.

Several methods, such as the structure tensor (Van Vliet & Verbeek 1995; Weickert 1997; Fehmers & Höcker 2003), coherence scanning (Marfurt 2006), plane-wave destruction (Fomel 2002) and dynamic image warping (Arias 2016), have been proposed to estimate seismic reflector orientations. However, the later three methods are not applicable to estimate orientations of seismic stratigraphic features such as channels. In this paper, we first discuss how to use the conventional structure-tensor method to estimate orientations of both structural features (reflections) and stratigraphic features (channels). We then discuss how to improve the estimation of seismic structural and stratigraphic orientations using directional structure tensors.

Assume $\mathbf{u}(\mathbf{x})$ is a unit vector normal to image features at the image sample $\mathbf{x}$. In an ideal image without noise, the gradient vector $\mathbf{g}(\mathbf{x})$ of the image should be parallel to the normal vector $\mathbf{u}$, along which the features vary most significantly. Practically, the image gradient vector, however, is often an unstable estimation of the true normal vector because of noise or measurement errors. Therefore, in practice we estimate the orientations of image features by fitting the gradient vectors in least-squares sense. Let $\mathbf{y}$ be a sample located in the neighbourhood Ω of the sample $\mathbf{x}$. The error of a gradient vector $\mathbf{g}(\mathbf{y})$ at a nearby sample $\mathbf{y}$ with respect to the normal vector $\mathbf{u}(\mathbf{x})$ can be defined as (van de Weijer 2005):

$$e(\mathbf{x},\mathbf{y}) = \|\mathbf{g}(\mathbf{y}) - [\mathbf{g}(\mathbf{y})^\top \mathbf{u}(\mathbf{x})]\mathbf{u}(\mathbf{x})\|, \tag{1}$$

where the difference $\mathbf{g}(\mathbf{y}) - [\mathbf{g}(\mathbf{y})^\top \mathbf{u}(\mathbf{x})]\mathbf{u}(\mathbf{x})$ is the projection of $\mathbf{g}$ on the normal to $\mathbf{u}$, and the error measures the normal distance from the gradient vector to the normal vector $\mathbf{u}$. The normal vector $\mathbf{u}(\mathbf{x})$ fitting all the gradients $\mathbf{g}(\mathbf{y})$ in the neighbourhood Ω of $\mathbf{x}$ can be computed by minimizing the following summation of weighted squared errors over all nearby samples:

$$E(\mathbf{x}) = \int_\Omega e^2(\mathbf{x},\mathbf{y}) G(\mathbf{x}-\mathbf{y}) \mathrm{d}\mathbf{y}, \tag{2}$$

where $G(\cdot)$ represents a Gaussian function (centred at $\mathbf{x}$), the aperture of which defines the neighbourhood of the sample $\mathbf{x}$. This equation can be rewritten as:

$$E(\mathbf{x}) = \int_\Omega \mathbf{g}^\top \mathbf{g} G \mathrm{d}\mathbf{y} - \int_\Omega \mathbf{u}^\top (\mathbf{g}\mathbf{g}^\top)\mathbf{u} G \mathrm{d}\mathbf{y}. \tag{3}$$

Minimizing this objective function is equivalent to solving the following constrained maximization problem:

$$\mathbf{u}^\top \left(\int_\Omega (\mathbf{g}\mathbf{g}^\top) G \mathrm{d}\mathbf{y} \right) \mathbf{u}, \text{ subject to } \mathbf{u}^\top \mathbf{u} = 1, \tag{4}$$

where $\mathbf{T}(\mathbf{x}) = \int_\Omega (\mathbf{g}\mathbf{g}^\top) G \mathrm{d}\mathbf{y}$ is the structure tensor which can be considered as smoothed outer products of gradient vectors in the neighbourhood centred at $\mathbf{x}$. To find the $\mathbf{u}$ that maximizes the above constrained objective function, we need to find the extrema of the function $\lambda(1 - \mathbf{u}^\top \mathbf{u}) + \mathbf{u}^\top \mathbf{T}\mathbf{u}$ according to the method of Lagrange multipliers. Differentiating this function with respect to $\mathbf{u}$ and letting the derivative to be zero, we have $\mathbf{T}\mathbf{u} = \lambda \mathbf{u}$, which indicates that the orientation vector $\mathbf{u}$ maximizing the objective function is the eigenvector of the structure tensor $\mathbf{T}$ corresponding to the largest eigenvalue.

For a 3-D image, each structure tensor $\mathbf{T}$ is a 3×3 symmetric positive-semi-definite matrix

$$\mathbf{T} = \langle \mathbf{g}\mathbf{g}^\top \rangle = \begin{bmatrix} \langle g_1 g_1 \rangle & \langle g_1 g_2 \rangle & \langle g_1 g_3 \rangle \\ \langle g_1 g_2 \rangle & \langle g_2 g_2 \rangle & \langle g_2 g_3 \rangle \\ \langle g_1 g_3 \rangle & \langle g_2 g_3 \rangle & \langle g_3 g_3 \rangle \end{bmatrix}, \tag{5}$$

where g_1, g_2 and g_3 are the three components of an image gradient vector $\mathbf{g}$ computed at a 3-D image sample. $\langle \cdot \rangle$ denotes Gaussian smoothing of whatever is inside the angle brackets. The eigendecomposition of such a 3-D structure tensor is as follows:

$$\mathbf{T} = \lambda_u \mathbf{u}\mathbf{u}^\top + \lambda_v \mathbf{v}\mathbf{v}^\top + \lambda_w \mathbf{w}\mathbf{w}^\top, \tag{6}$$

where $\mathbf{u}$, $\mathbf{v}$ and $\mathbf{w}$ are normalized eigenvectors corresponding to the eigenvalues λ_u, λ_v and λ_w, respectively. These eigenvectors provide an estimation of orientations of consistent features in the 3-D image. For a 3-D seismic image, these eigenvectors can be used to approximate the orientations of structural and stratigraphic features such as reflections and channels.

2.1 Seismic structural orientations

As discussed by Hale (2009b), if we label the eigenvalues $\lambda_u \geq \lambda_v \geq \lambda_w \geq 0$, then the corresponding eigenvectors $\mathbf{u}$ are parallel to directions in which the image features vary most significantly; while the eigenvectors $\mathbf{w}$ are parallel to directions in which the image features vary least significantly. Both eigenvectors $\mathbf{v}$ and $\mathbf{w}$ lie within local planes of planar image features. Therefore, in a

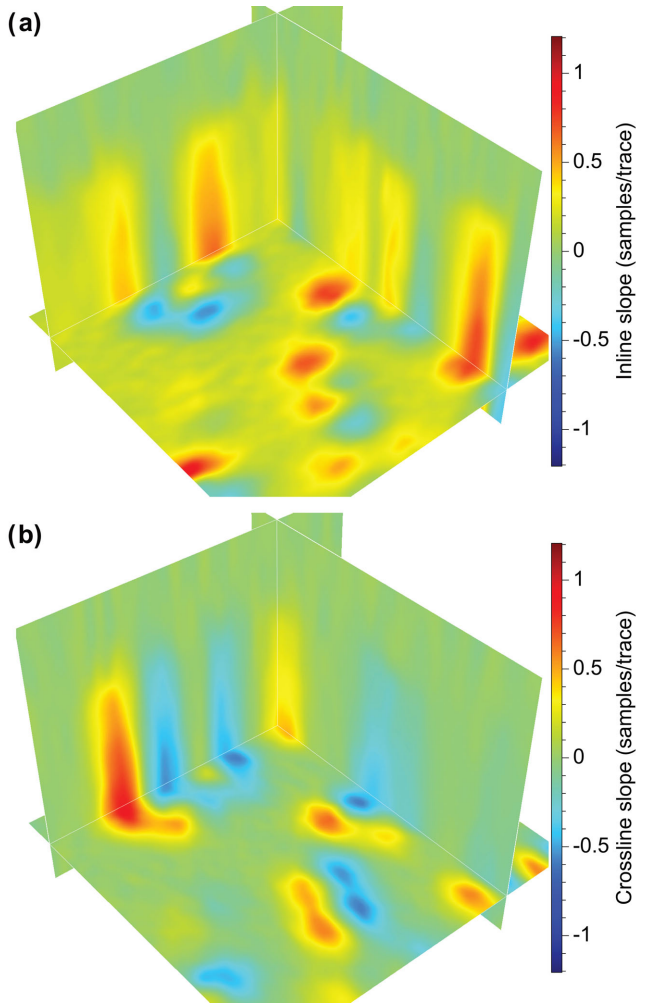

Figure 3. Estimated inline (a) and crossline (b) slopes using the conventional structure-tensor method.

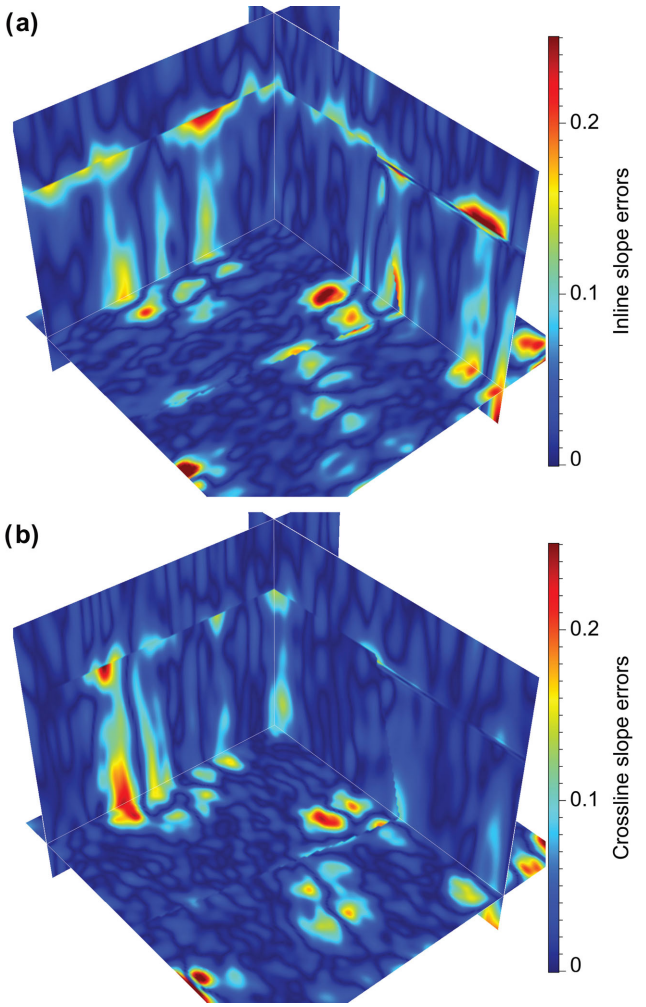

Figure 4. Absolute errors of the estimated inline (a) and crossline (b) slopes using the conventional structure-tensor method.

3-D seismic image, the normal vectors of seismic reflections can be approximated by the eigenvectors $\mathbf{u}$, and the vectors parallel to seismic stratigraphic features (channels) can be approximated by the eigenvectors $\mathbf{w}$.

In 3-D cases, the normalized eigenvectors $\mathbf{u}$ are unit vectors that contain three components $\mathbf{u} = (u_1, u_2, u_3)$, where u_1, u_2, and u_3 represent vertical, inline, and crossline components, respectively. As reflections are rarely vertical, we can assume the reflection normals are always pointing downward and the vertical components $u_1 > 0$. The inline and crossline slopes s_2 and s_3 of seismic reflectors can be computed from the eigenvectors $\mathbf{u}$ as follows:

$$s_2 = -\frac{u_2}{u_1} \quad \text{and} \quad s_3 = -\frac{u_3}{u_1}. \tag{7}$$

Figs 3(a) and (b) show the inline (s_2) and crossline (s_3) slopes computed from the eigenvectors $\mathbf{u}$ of the conventional structure tensors (eq. 5). These estimated slopes (Fig. 3) look similar to the true slopes (Figs 1b and c). However, significant errors or residuals are existing in these estimated slopes as shown in the images of absolute differences between the true and estimated slopes in Fig. 4. These residuals are relatively higher in areas where the slopes vary faster.

The residuals are mainly generated by noise in the seismic image and the smoothing in constructing structure tensors. In a clean image without noise, the gradient vectors $\mathbf{g}$ of the image will be an ideal estimation of the orientations perpendicular to seismic reflections. In practice, the gradient vectors are noisy and are not necessarily perpendicular to seismic reflections. Therefore, we expect to compute more stable average orientations by applying some smoothing filter to each element of the gradient-based structure tensors as shown in eq. (5). The smoothing is helpful to compute stable orientations, however, may reduce the resolution of orientation variation in an image. In computing the slopes shown in Fig. 3, we implemented the smoothing in eq. (5) as a Gaussian filter and the smoothing extents (or half width) in vertical, inline, and crossline directions are $\sigma_1 = 8$ (samples), $\sigma_2 = 2$ (samples), and $\sigma_3 = 2$ (samples), respectively. These smoothing parameters are the optimal ones for this example to compute the best slope estimation (Fig. 3) with the smallest absolute errors (Fig. 4), which are still significant in some areas with steep and highly varying slopes.

2.2 Seismic stratigraphic orientations

The spatial orientations of the seismic channel (Fig. 2a) can be approximated by the eigenvectors $\mathbf{w} = (w_1, w_2, w_3)$ computed from the structure tensors. Since the eigenvectors $\mathbf{u}$ are perpendicular to the channel, then we can also uniquely describe the orientations of the channel by using $\mathbf{u}$ and the lateral azimuth α shown in Fig. 2(a).

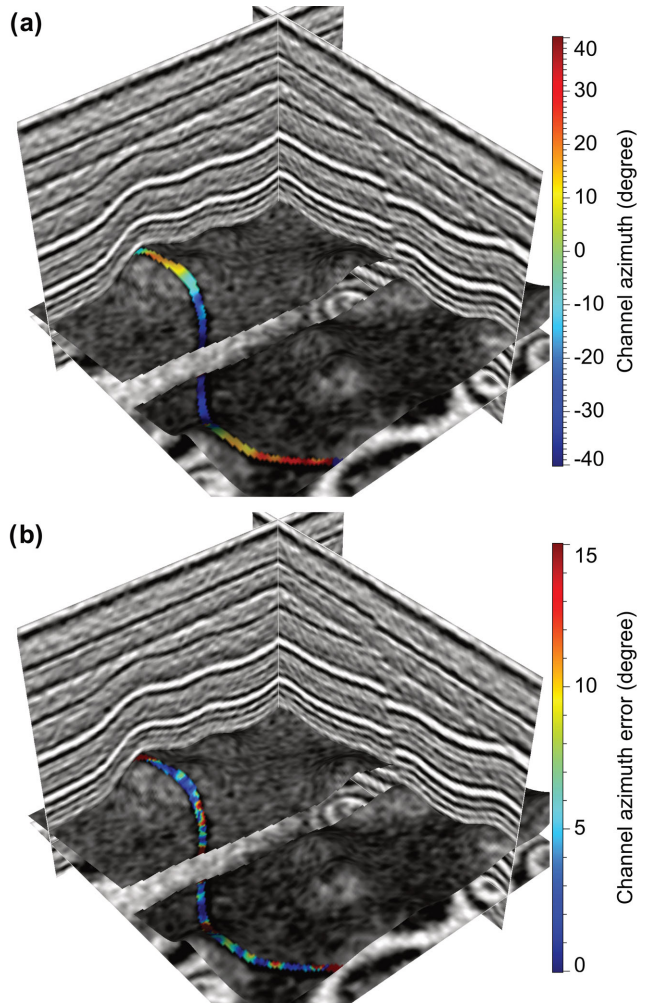

Figure 5. Channel azimuth (a) estimated using the conventional structure-tensor method and the absolute errors (b) of the estimated azimuth.

This lateral azimuth α can be computed from the inline (w_2) and crossline (w_3) components of the eigenvectors $\mathbf{w}$:

$$\alpha = \arctan \frac{w_3}{w_2}. \tag{8}$$

Fig. 5(a) shows the channel azimuth α values that are computed from the eigenvectors $\mathbf{w}$ of conventional structure tensors. We actually compute the azimuth values everywhere in the 3-D seismic image, but display those values only on the channel because the eigenvectors $\mathbf{w}$ in areas away from the channel are arbitrarily oriented along reflections. Fig. 5(b) shows the absolute errors of the estimated channel azimuth values compared to the true ones in Fig. 2(b). We observe that the errors in the estimated seismic channel orientations (Fig. 5b) are even bigger than those in the estimated reflection slopes (Fig. 4) by using the conventional structure tensors. In the next section, we will discuss how to improve both estimations of seismic structural and stratigraphic orientations.

3 DIRECTIONAL STRUCTURE TENSORS

To better estimate orientations of seismic structures (reflections), we compute 2-D or 3-D directional structure tensors with directional derivatives in directions perpendicular and parallel to reflections. By doing this, we actually construct structure tensors in a new space where reflections are flat or only slightly dipping. The orientations of such slightly dipping reflections can be accurately estimated in this new space and then transformed back to obtain an accurate estimation of the reflection orientations in the original space. In 3-D cases, to better estimate spatial orientations of seismic stratigraphic features (channels), we construct 2-D directional structure tensors with directional derivatives parallel to seismic reflections. Such directional structure tensors are equivalent to the conventional structure tensors computed along a horizon surface, and therefore are robust to estimate orientations of stratigraphic features that are aligned within dipping reflections.

3.1 Improved structural orientations

As discussed in the previous section, smoothing is required in constructing structure tensors to obtain stable orientation estimations but reduces the resolution of orientation variations. We therefore observe the largest errors apparent in areas with rapidly varying slopes as shown in Fig. 4. In addition, steep structures can easily generate alias in structure tensors as discussed by Köthe (2003), which can make the conventional structure tensors fail to accurately estimate the orientations of highly dipping structures. To avoid errors in estimating slopes of highly dipping and rapidly varying reflections, we propose to estimate reflections slopes in a new *upq* space, where the reflections are flat or slightly dipping and the slope variations are reduced. We define such a space by using reflection normals $\mathbf{u}$ estimated from the conventional structure tensors. In this *upq* space, the vertical curvilinear axis is locally parallel to the initial normals $\mathbf{u}$, while the other two curvilinear axes are locally parallel to unit vectors $\mathbf{p}$ and $\mathbf{q}$ that are orthogonal to $\mathbf{u}$ and laterally aligned within seismic reflections.

Assume the vectors $\mathbf{p}$ are locally parallel to reflections in the inline directions, and therefore can be considered as the reflection inline slope vectors, which can be computed as

$$\mathbf{p} = \begin{bmatrix} \frac{s_2}{\sqrt{s_2^2+1}} \\ \frac{1}{\sqrt{s_2^2+1}} \\ 0 \end{bmatrix} = \begin{bmatrix} \frac{-u_2}{\sqrt{u_1^2+u_2^2}} \\ \frac{u_1}{\sqrt{u_1^2+u_2^2}} \\ 0 \end{bmatrix}. \tag{9}$$

The vectors $\mathbf{p}$ are orthogonal to the approximate reflection normals $\mathbf{u}$, which indicates that $\mathbf{p}$ are locally approximately parallel to seismic reflections. In addition, the crossline components of $\mathbf{p}$ are zeros and the inline components are positive ($\frac{u_1}{\sqrt{u_1^2+u_2^2}} > 0$), which means that the axis following the vectors $\mathbf{p}$ is exactly aligned within the vertical-inline plane and always increases with the inline axis.

The other unit vectors $\mathbf{q}$ should be orthogonal to both vectors $\mathbf{u}$ and $\mathbf{p}$, and therefore can be computed as

$$\mathbf{q} = \begin{bmatrix} \frac{-u_1u_3}{\sqrt{(u_1^2+u_2^2)^2+(u_2u_3)^2+(u_1u_3)^2}} \\ \frac{-u_2u_3}{\sqrt{(u_1^2+u_2^2)^2+(u_2u_3)^2+(u_1u_3)^2}} \\ \frac{u_1^2+u_2^2}{\sqrt{(u_1^2+u_2^2)^2+(u_2u_3)^2+(u_1u_3)^2}} \end{bmatrix} = \begin{bmatrix} \frac{-u_1u_3}{\sqrt{u_1^2+u_2^2}} \\ \frac{-u_2u_3}{\sqrt{u_1^2+u_2^2}} \\ \frac{u_1^2+u_2^2}{\sqrt{u_1^2+u_2^2}} \end{bmatrix}. \tag{10}$$

Similar to the vectors $\mathbf{p}$, the vectors $\mathbf{q}$ are also orthogonal to the reflection normal vectors $\mathbf{u}$ and therefore are locally approximately parallel to reflections. Since the crossline components of $\mathbf{q}$ are always positive, then the axis following the vectors $\mathbf{q}$ always increases with the crossline axis. However, since the inline components of $\mathbf{q}$

are not necessarily equal to zeros, then the vectors **q** are not crossline slope vectors, and the axis following the vectors **q** is not necessarily aligned within the vertical-crossline plane.

The new *upq* space spanned by these three orthogonal vectors **u**, **p** and **q** is similar to the *uvt* space discussed by Mallet (2002, 2004). In this space, the axes u, p, and q locally follows the vectors **u**, **p** and **q**, respectively, and therefore are curvilinear. The u axis is locally perpendicular to seismic reflections and always increases ($u_1 > 0$) with the vertical time- or depth-axis. The p and q axes are aligned within seismic reflections and always increases ($p_2 > 0$ and $q_3 > 0$) with the inline and crossline axes, respectively. Ideally, seismic reflections in this *upq* space should be all flat as in the *uvt* space. In practice, reflections might be still slightly dipping because the estimated reflection normals **u** may not be accurately perpendicular to reflections and the vectors **p** and **q** may not be accurately aligned within the reflections. However, it is still helpful to consider the estimation of reflection orientations in the new space because the reflections are mostly flat or only slightly dipping and the slope variations are reduced in this space. Orientations of such slightly dipping reflections in this new space can be accurately estimated by using structure tensors.

To estimate reflection orientations in the new space, we do not need to explicitly transform the whole seismic image into this space. We only need to compute local derivatives in directions along the vectors **u**, **p** and **q** and use them to construct 3-D directional structure tensors as follows:

$$\mathbf{T}_d = \begin{bmatrix} \langle g_u g_u \rangle & \langle g_u g_p \rangle & \langle g_u g_q \rangle \\ \langle g_u g_p \rangle & \langle g_p g_p \rangle & \langle g_p g_q \rangle \\ \langle g_u g_q \rangle & \langle g_p g_q \rangle & \langle g_q g_q \rangle \end{bmatrix}, \tag{11}$$

where g_u, g_p and g_q represent directional derivatives of a 3-D seismic image in directions along the orthogonal unit vectors **u**, **p** and **q**, respectively. Note that these directional derivatives $g_u(\mathbf{x})$, $g_p(\mathbf{x})$, and $g_q(\mathbf{x})$ and the directional structure tensors $\mathbf{T}_d(\mathbf{x})$ are computed on the sampling grid of the seismic image $f(\mathbf{x})$ in the original space $\mathbf{x} = (x_1, x_2, x_3)$. Interpolations are required to compute the directional derivatives:

$$\begin{aligned} g_u(\mathbf{x}) &= \frac{1}{2}\left[f(\mathbf{x}+\mathbf{u}(\mathbf{x})) - f(\mathbf{x}-\mathbf{u}(\mathbf{x}))\right] \\ g_p(\mathbf{x}) &= \frac{1}{2}\left[f(\mathbf{x}+\mathbf{p}(\mathbf{x})) - f(\mathbf{x}-\mathbf{p}(\mathbf{x}))\right] \\ g_q(\mathbf{x}) &= \frac{1}{2}\left[f(\mathbf{x}+\mathbf{q}(\mathbf{x})) - f(\mathbf{x}-\mathbf{q}(\mathbf{x}))\right], \end{aligned} \tag{12}$$

where $f(\mathbf{x} \pm \mathbf{u}(\mathbf{x}))$, $f(\mathbf{x} \pm \mathbf{p}(\mathbf{x}))$ and $f(\mathbf{x} \pm \mathbf{q}(\mathbf{x}))$ are interpolated from the input seismic image $f(\mathbf{x})$ using the sinc interpolation method.

Ideally, the smoothing $\langle \cdot \rangle$ in eq. (11) should be implemented as structure-oriented smoothing (Fehmers & Höcker 2003; Hale 2009b) in directions along vectors **u**, **p** and **q**. However, as discussed previously in this paper, this smoothing only provides a weighted average of the neighbouring orientations. Therefore, to be efficient, we can still implement such a weighted average with a Gaussian smoothing in vertical, inline, and crossline directions. To be consistent, the smoothing extents in constructing these directional structure tensors (eq. 11) are the same as in constructing the conventional structure tensors (eq. 5).

By using the directional derivatives in directions along **u**, **p** and **q**, we actually construct the directional structure tensors in the new space spanned by vectors **u**, **p** and **q**. In this space, reflections are flat or only slightly dipping, the eigenvectors $\hat{\mathbf{u}}$ (corresponding to the maximum eigenvalues) of the structure tensors (eq. 11) can often provide an accurate estimation of the normals of these reflections. However, these eigenvectors $\hat{\mathbf{u}}$ are computed in the new space spanned by **u**, **p**, and **q**. We need to transform $\hat{\mathbf{u}}$ back to the original vertical–inline–crossline space and obtain an estimation of reflection normals $\tilde{\mathbf{u}}$ in the original space:

$$\tilde{\mathbf{u}} = [\mathbf{u}\ \mathbf{p}\ \mathbf{q}]\hat{\mathbf{u}} = \begin{bmatrix} u_1 & \dfrac{-u_2}{\sqrt{u_1^2+u_2^2}} & \dfrac{-u_1u_3}{\sqrt{u_1^2+u_2^2}} \\ u_2 & \dfrac{u_1}{\sqrt{u_1^2+u_2^2}} & \dfrac{-u_2u_3}{\sqrt{u_1^2+u_2^2}} \\ u_3 & 0 & \dfrac{u_1^2+u_2^2}{\sqrt{u_1^2+u_2^2}} \end{bmatrix} \begin{bmatrix} \hat{u}_u \\ \hat{u}_p \\ \hat{u}_q \end{bmatrix}. \tag{13}$$

If the initial reflection normals **u** are all accurately perpendicular to the seismic reflections, then the reflections should be all flat and we will have $\hat{\mathbf{u}} = (1, 0, 0)$ in the new space spanned by **u**, **p** and **q**. Then we have $\tilde{\mathbf{u}} = \mathbf{u}$ according to the transformation eq. (13), which means that we will have no updates in the new unit vectors $\tilde{\mathbf{u}}$. If there are errors or residuals existing in the initial normals **u**, that is, **u** are not perfectly perpendicular to the reflections, then there will be slightly dipping reflections in the new space. The estimated $\hat{\mathbf{u}}$ ($\hat{\mathbf{u}} \neq (1, 0, 0)$) will be perpendicular to these dipping reflections in the new space, and the transformed unit vectors $\tilde{\mathbf{u}}$ ($\tilde{\mathbf{u}} \neq \mathbf{u}$) are supposed to correct the potential residuals in **u**. The estimated new reflection normals $\tilde{\mathbf{u}}$ are supposed to be more accurate than the initial normals **u** because the structure-tensor method is more reliable to estimate normals of reflections with small and slowly varying slopes in the new space than those with high and rapidly varying slopes in the original space.

Fig. 6 shows the p-axis (Fig. 6a) and q-axis (Fig. 6b) slopes of reflections computed in the *upq* space. We compute these p-axis slope s_p and q-axis slope s_q from the eigenvectors $\hat{\mathbf{u}}$ of the structure tensors (eq. 11) in the new space:

$$s_p = -\frac{\hat{u}_p}{\hat{u}_u} \quad \text{and} \quad s_q = -\frac{\hat{u}_q}{\hat{u}_u}. \tag{14}$$

We observe the reflection slopes s_p (Fig. 6a) and s_q (Figs 6b), estimated in the new space, are close to zero and vary slowly within a small range from -0.5 to 0.5. In addition, the relatively high values in s_p and s_q appear in areas where the errors (Fig. 4) are relatively high in the initially estimated reflection slopes (Fig. 3) or the corresponding normals **u**. These observations are consistent with what we expect because the reflections in the new space should be flat in most areas and be slightly dipping only in areas where the initially estimated reflection slopes or normals are not accurate enough.

Fig. 7 shows the new inline and crossline slopes $\tilde{s}_2$ and $\tilde{s}_3$ computed from $\tilde{\mathbf{u}}$:

$$\tilde{s}_2 = -\frac{\tilde{u}_2}{\tilde{u}_1} \quad \text{and} \quad \tilde{s}_3 = -\frac{\tilde{u}_3}{\tilde{u}_1}. \tag{15}$$

Fig. 8 shows the corresponding absolute errors of the new slopes compared to the true slopes in Fig. 1. These absolute errors in the new slopes are significantly decreased compared to those in the previous slopes (Fig. 4) computed from the conventional structure tensors. In Fig. 8, we still observe significant errors near the unconformity and fault where the true slopes (Fig. 1) are discontinuous. This is because we still apply smoothing across the unconformity and fault in constructing the directional structure tensors (eq. 11). These errors might be further corrected by first detecting fault and unconformity surfaces from the seismic image, and use these

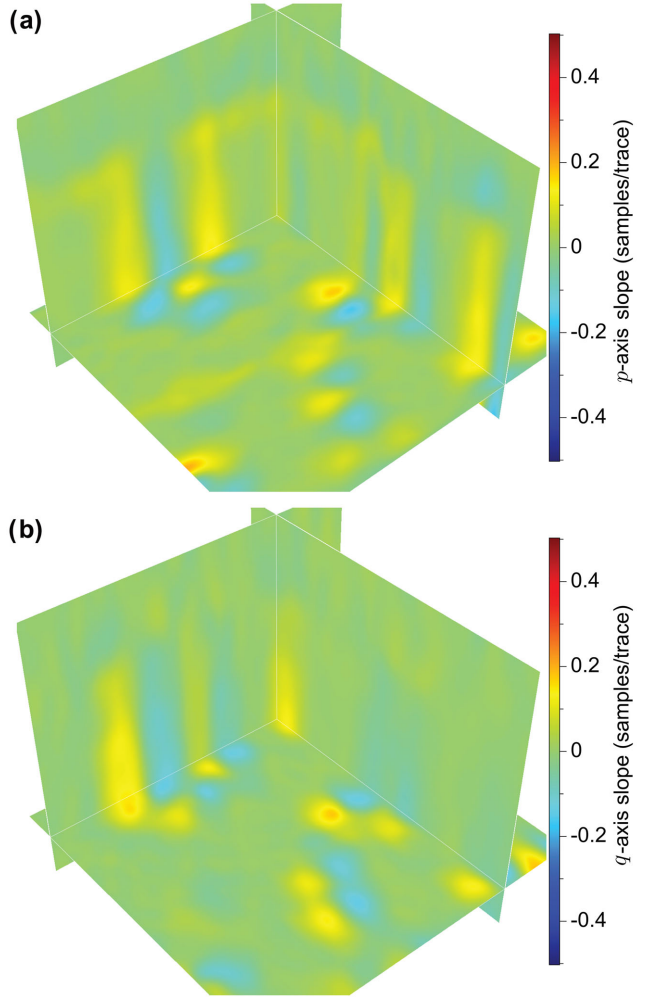

Figure 6. p-axis (a) and q-axis (b) slopes estimated in the new upq space, where reflections are flat or only slightly dipping and slope variations are reduced.

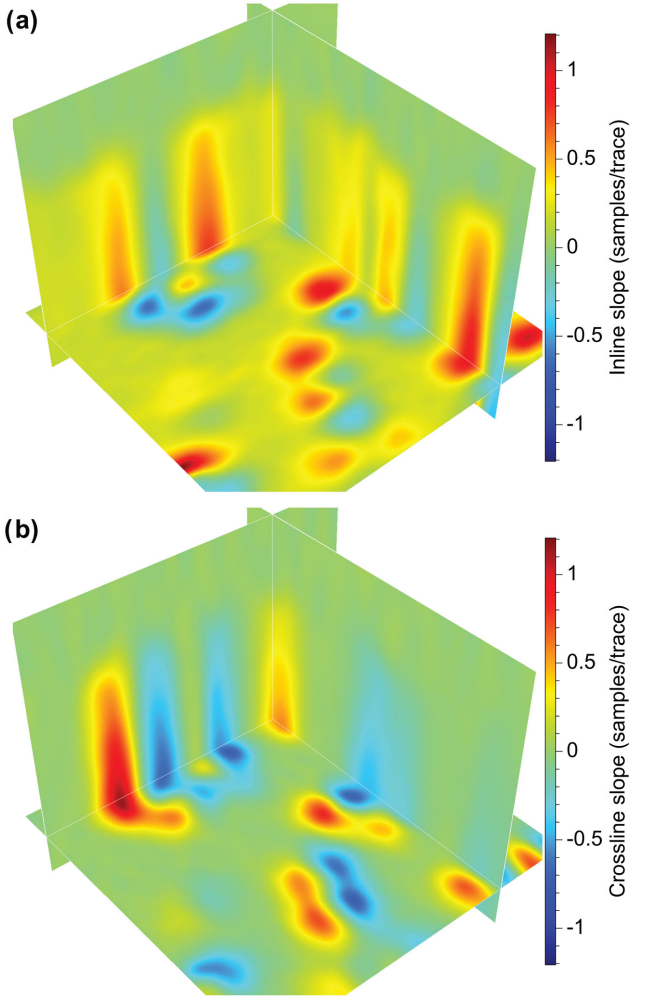

Figure 7. The slopes (Fig. 6) estimated in the new space are transformed back to obtain the inline (a) and crossline (b) slopes in the original space.

surfaces as input constraints to stop the smoothing near the faults and unconformities, as discussed by Wu & Hale (2015a).

3.2 Improved stratigraphic orientations

A straightforward way to estimate orientations of seismic stratigraphic features is to first extract stratigraphic surfaces (horizons) from a 3-D seismic image by following reflections, and then try to estimate the orientations of the stratigraphic features apparent on each horizon surface. Specifically, one can compute 2-D gradients of seismic amplitudes on a horizon surface, and use the gradients to construct 2-D conventional structure tensors to estimate the stratigraphic orientations as discussed by Hale (2009b). Using amplitude gradients computed along a horizon surface to construct structure tensors, we are able to better capture the stratigraphic features in the structure tensors compared to using vertical and horizontal derivatives in the conventional 3-D structure tensors (eq. 5). Therefore, stratigraphic orientations estimated in this way should be more accurate than those ($\mathbf{w}$) computed from the 3-D conventional structure tensors (eq. 5). However, the disadvantage of this straightforward way is that it requires first extracting all horizon surfaces from a 3-D seismic image, which can be difficult and time-consuming in practice.

Fortunately, computing amplitude gradients along a horizon surface is only a local operation, which actually does not require first extracting the surface. As a horizon surface often follows seismic reflections, the equivalent amplitude gradients can be simply computed from directional derivatives of a 3-D seismic image in directions parallel to the reflections. Based on this observation, we propose a more efficient but equivalent way to construct 2-D structure tensors for estimating stratigraphic orientations.

In this method, we do not need to first extract horizon surfaces from a 3-D seismic image, instead, we only need to first estimate reflection normals $\tilde{\mathbf{u}}$ (eq. 13). From the reflection normals, we compute the corresponding orthogonal vectors $\tilde{\mathbf{p}}$ and $\tilde{\mathbf{q}}$ (eqs 9 and 10) that are orthogonal to $\tilde{\mathbf{u}}$ and aligned within seismic reflections. We then use the vectors $\tilde{\mathbf{p}}$ and $\tilde{\mathbf{q}}$ to construct 2-D structure tensors of stratigraphic features as

$$\mathbf{T}_s = \begin{bmatrix} \langle g_{\tilde{p}} g_{\tilde{p}} \rangle_s & \langle g_{\tilde{p}} g_{\tilde{q}} \rangle_s \\ \langle g_{\tilde{p}} g_{\tilde{q}} \rangle_s & \langle g_{\tilde{p}} g_{\tilde{q}} \rangle_s \end{bmatrix}, \tag{16}$$

where g_p and g_q are locally directional derivatives computed along seismic reflections in directions of vectors $\tilde{\mathbf{p}}$ and $\tilde{\mathbf{q}}$, respectively. $\langle\cdot\rangle_s$ represents structure-oriented smoothing in directions along the vectors $\tilde{\mathbf{u}}$, $\tilde{\mathbf{p}}$ and $\tilde{\mathbf{q}}$. We implement this smoothing with anisotropic diffusion (Weickert 1997, 1999), and the smoothing extents in directions of $\tilde{\mathbf{u}}$, $\tilde{\mathbf{p}}$ and $\tilde{\mathbf{q}}$ are approximately equal to 1 (samples), 4

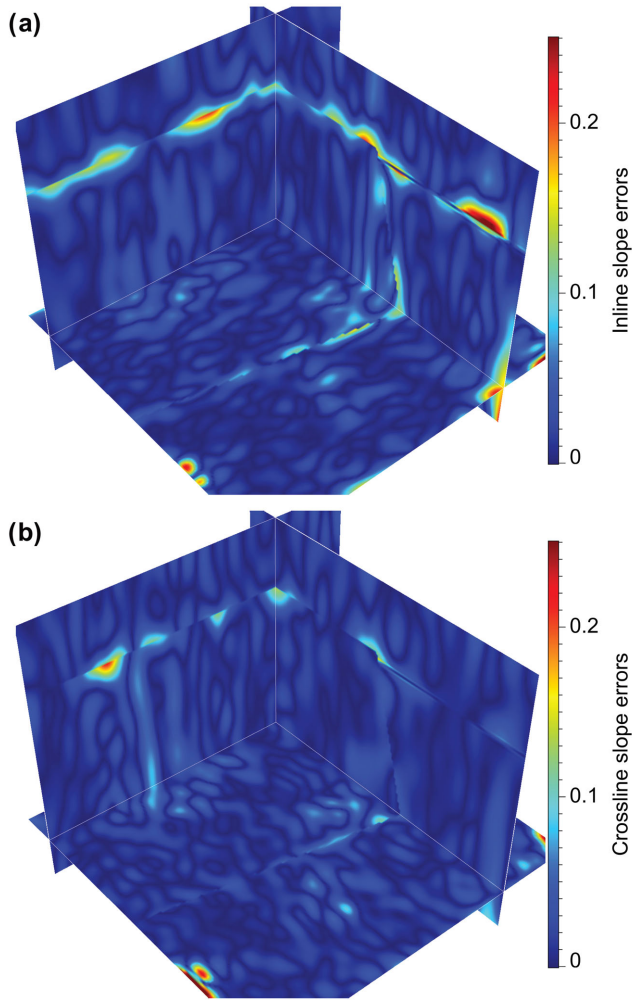

Figure 8. Absolute errors of the estimated inline (a) and crossline (b) slopes using the directional structure tensors.

(samples) and 4 (samples), respectively, for the synthetic example. We generally apply much stronger smoothing in lateral directions ($\tilde{\mathbf{p}}$ and $\tilde{\mathbf{q}}$) than the normal directions ($\tilde{\mathbf{u}}$) because the stratigraphic features are linear features that are mainly elongated laterally along reflections. This is also the reason why we cannot simply implement the smoothing with a Gaussian smoothing filter in vertical and horizontal directions.

By computing amplitude derivatives along seismic reflections, seismic structures or reflections are removed or destructed (Fomel 2002) and only the information of stratigraphic features are captured within these directional derivatives. Therefore, using the directional derivatives, we actually construct structure tensors of the stratigraphic features aligned within the dipping reflections. From these structure tensors, we further compute the corresponding eigendecompositions as follows to estimate the stratigraphic orientations:

$$\mathbf{T}_s = \lambda_a \mathbf{a}\mathbf{a}^\top + \lambda_b \mathbf{b}\mathbf{b}^\top, \tag{17}$$

where λ_a and λ_b ($\lambda_a \geq \lambda_b$) are eigenvalues, and $\mathbf{a} = (a_{\tilde{p}}, a_{\tilde{q}})$ and $\mathbf{b} = (b_{\tilde{p}}, b_{\tilde{q}})$ are corresponding 2-D eigenvectors. These eigenvectors $\mathbf{a}$ and $\mathbf{b}$ indicate how the stratigraphic features are laterally oriented along reflections in the 2-D $\tilde{p}\tilde{q}$ space. We can transform these vectors back to the original inline–crossline space as

$$\tilde{\mathbf{a}} = \begin{bmatrix} \tilde{p}_2 & \tilde{q}_2 \\ \tilde{p}_3 & \tilde{q}_3 \end{bmatrix} \begin{bmatrix} a_{\tilde{p}} \\ a_{\tilde{q}} \end{bmatrix} \text{ and } \tilde{\mathbf{b}} = \begin{bmatrix} \tilde{p}_2 & \tilde{q}_2 \\ \tilde{p}_3 & \tilde{q}_3 \end{bmatrix} \begin{bmatrix} b_{\tilde{p}} \\ b_{\tilde{q}} \end{bmatrix}, \tag{18}$$

where the inline ($\tilde{p}_2$ and $\tilde{q}_2$) and crossline ($\tilde{p}_3$ and $\tilde{q}_3$) components of vectors $\tilde{\mathbf{p}}$ and $\tilde{\mathbf{q}}$ are computed from the reflection normal vectors $\tilde{\mathbf{u}}$ according to eqs (9) and (10). The transformed vectors $\tilde{\mathbf{a}}$ and $\tilde{\mathbf{b}}$ indicate how the stratigraphic features are laterally oriented in the original inline–crossline space. Specifically, if we vertically project the 3-D oriented stratigraphic features (e.g. channels) to the 2-D horizontal inline–crossline space, then the eigenvectors $\tilde{\mathbf{a}}$ and $\tilde{\mathbf{b}}$, respectively, are approximately perpendicular and parallel to the stratigraphic features projected in the 2-D horizontal space. Both the eigenvectors $\tilde{\mathbf{a}} = (\tilde{a}_2, \tilde{a}_3)$ and $\tilde{\mathbf{b}} = (\tilde{b}_2, \tilde{b}_3)$ contain only the inline ($\tilde{a}_2$ and $\tilde{b}_2$) and crossline ($\tilde{a}_3$ and $\tilde{b}_3$) components of the stratigraphic orientations.

To describe the orientations of stratigraphic features in 3-D space, we can compute vectors $\tilde{\mathbf{v}} = (\tilde{v}_1, \tilde{v}_2, \tilde{v}_3)$ and $\tilde{\mathbf{w}} = (\tilde{w}_1, \tilde{w}_2, \tilde{w}_3)$ that are perpendicular and parallel to the stratigraphic features in 3-D space by using the vectors $\tilde{\mathbf{u}}$, $\tilde{\mathbf{a}}$, and $\tilde{\mathbf{b}}$. As the vectors $\tilde{\mathbf{v}}$ and $\tilde{\mathbf{w}}$ will be aligned within seismic reflections, both of them should be orthogonal to the vectors $\tilde{\mathbf{u}}$: $\tilde{\mathbf{u}}^\top \tilde{\mathbf{v}} = \tilde{\mathbf{u}}^\top \tilde{\mathbf{w}} = 0$. Therefore, the three components of vectors $\tilde{\mathbf{v}}$ can be computed as

$$\tilde{v}_3 = \tilde{a}_3, \quad \tilde{v}_2 = \tilde{a}_2 \quad \text{and} \quad \tilde{v}_1 = -\frac{\tilde{u}_2\tilde{a}_2 + \tilde{u}_3\tilde{a}_3}{\tilde{u}_1}. \tag{19}$$

Similarly, the three components of $\tilde{\mathbf{w}}$ can be computed as

$$\tilde{w}_3 = \tilde{b}_3, \quad \tilde{w}_2 = \tilde{b}_2 \quad \text{and} \quad \tilde{w}_1 = -\frac{\tilde{u}_2\tilde{b}_2 + \tilde{u}_3\tilde{b}_3}{\tilde{u}_1}. \tag{20}$$

We can further normalize the vectors $\tilde{\mathbf{v}}$ and $\tilde{\mathbf{w}}$ by $\sqrt{\tilde{v}_1^2 + \tilde{v}_2^2 + \tilde{v}_3^2}$ and $\sqrt{\tilde{w}_1^2 + \tilde{w}_2^2 + \tilde{w}_3^2}$, respectively, to obtain corresponding unit vectors that are locally perpendicular and parallel to seismic stratigraphic features in the 3-D space.

The lateral azimuth $\tilde{\alpha}$ (Fig. 2a) of the stratigraphic features (channels) can be estimated from the two components of the vectors $\tilde{\mathbf{b}}$ or the inline and crossline components of the vectors $\tilde{\mathbf{w}}$:

$$\tilde{\alpha} = \arctan\frac{\tilde{b}_3}{\tilde{b}_2} = \arctan\frac{\tilde{w}_3}{\tilde{w}_2}. \tag{21}$$

The RGB colours in Fig. 9(a) shows the estimated lateral azimuth of the channel in the synthetic example, which looks almost the same as the true azimuth shown in Fig. 2(b). Fig. 9(b) shows the corresponding absolute errors, which are significantly reduced compared to the errors (Fig. 5b) in the azimuth (Fig. 5a) estimated using the 3-D conventional structure tensors.

In Fig. 9(a), We display the azimuth of stratigraphic features only at the channel on the surface because there is no linear stratigraphic features in areas away from the channel. In these areas, the image features are isotropic and therefore the vectors $\tilde{\mathbf{v}}$ and $\tilde{\mathbf{w}}$ are arbitrarily oriented within the horizon surface. In addition, we estimated the stratigraphic azimuth without picking the horizon surface, we compute the azimuth at each image sample directly from the 3-D seismic image using the directional structure tensors defined in eq. (16).

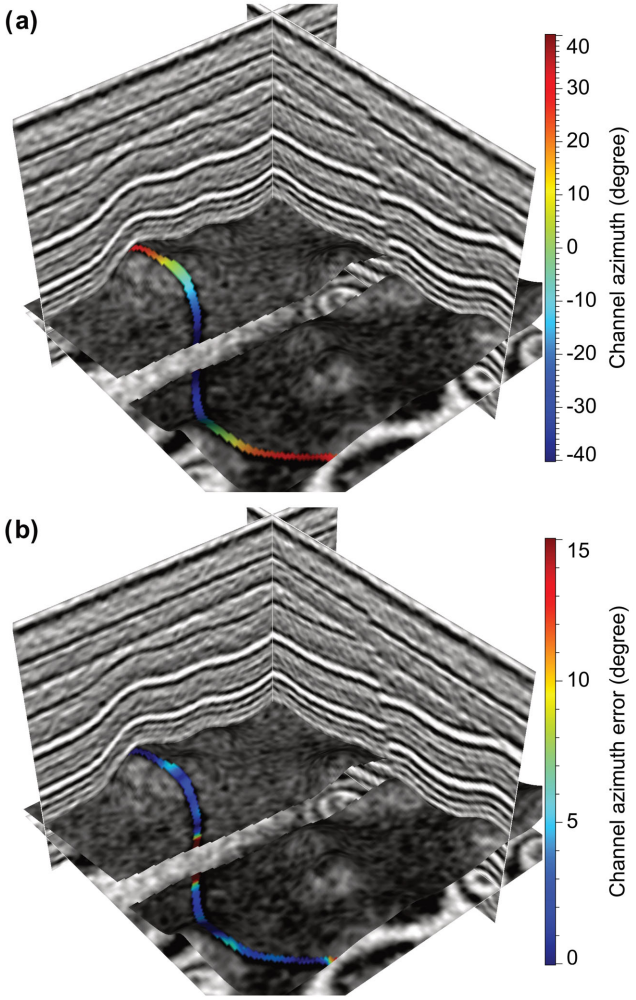

Figure 9. Channel azimuth (a) estimated using the improved structure-tensor method and the absolute errors (b) of the estimated azimuth.

4 REAL EXAMPLES

The synthetic 3-D example shown in Figs 1–9 illustrates the methods of using directional structure tensors to better estimate seismic structural and stratigraphic orientations. To further demonstrate the methods, we apply them to two real 3-D seismic images with steep structures (reflections) and many stratigraphic features (channels).

4.1 Structural orientations

To demonstrate how the directional structure tensors can better estimate structural orientations than the conventional structure tensors, we use the real 3-D Poseidon seismic image with complicated carbonates as shown in Fig. 10. The upper-right panel in Fig. 10 shows a zoomed in 3-D view of the seismic image, while the upper-left, lower-left, and lower-right panels, respectively, display the time, crossline, and inline slices extracted from the whole 3-D seismic image. This Poseidon seismic image shows a small Miocene isolated carbonate platform that progrades into deeper outer shelf area on the Browse basin of the NW Shelf of Australia (Howarth & Alves 2016). The lateral accretion of the isolated carbonate platform is represented by sigmoidal reflection package. The internal reflection geometry in those sigmoid includes shingling steep inclined reflections associated with donwlap, downdip and truncation updip. The reflection slopes are highly steep inside the carbonates and the slopes vary rapidly in both vertical and horizontal directions. The conventional structure tensors often yield significant errors in estimating such steep slopes with rapid variations.

Figs 11(a) and 12(a), respectively, show the inline and crossline slopes s_2 and s_3 that are computed from the eigenvectors $\mathbf{u}$ of the 3-D conventional structure tensors (eq. 5). In constructing the conventional structure tensors, we apply Gaussian smoothing to each element of the tensors, and the smoothing extents in vertical, inline, and crossline directions are $\sigma_1 = 8$ (samples), $\sigma_2 = 2$ (samples), and $\sigma_3 = 2$ (samples), respectively.

With these estimated reflection normals $\mathbf{u}$, we compute the corresponding orthogonal vectors $\mathbf{p}$ and $\mathbf{q}$, and then compute directional derivatives in directions along these three vectors. We further use these directional derivatives to construct directional structure tensors in the *upq* space as in eq. (11). In constructing such directional structure tensors, we apply exactly the same Gaussian smoothing to each element of the tensors in vertical, inline, and crossline directions. From the directional structure tensors, we first compute normal vectors $\hat{\mathbf{u}}$ of reflections in the new space spanned by the orthogonal vectors $\mathbf{u}$, $\mathbf{p}$, and $\mathbf{q}$. We then transform (eq. 13) the eigenvectors $\hat{\mathbf{u}}$ back to obtain reflection normals $\tilde{\mathbf{u}}$ in the original vertical–inline–crossline space. Figs 11(b) and 12(b), respectively, show the new inline and crossline slopes computed from the vectors $\tilde{\mathbf{u}}$.

As shown in Figs 11 and 12, the new slopes (Figs 11b and 12b) are much different from the conventional slopes (Figs 11a and 12a) inside the carbonates with steep and rapidly varying slopes. Inside the carbonates, the absolute values of the new slopes are relatively higher than the conventional slopes, which may indicate the new slopes are closer to the true slopes of the steep reflections inside the carbonates.

To verify the estimated slopes, we use them in a slope-based horizon tracking method to extract horizons, which should follow seismic reflections if the input slopes are accurate enough. Numerous slope-based methods (de Groot *et al.* 2006; Lomask *et al.* 2006; Parks 2010; Fomel 2010; Luo & Hale 2013; Wu & Hale 2015b) have been proposed to extract horizons using reflections slopes. We use the method discussed by Wu & Hale (2013, 2015b) to verify the slopes in this paper. In this method, a horizon surface $f(x, y)$ is iteratively computed by solving the following nonlinear equation

$$\begin{bmatrix} \partial f^i(x,y)/\partial x \\ \partial f^i(x,y)/\partial y \end{bmatrix} \approx \begin{bmatrix} s_2(x,y,f^{i-1}(x,y)) \\ s_3(x,y,f^{i-1}(x,y)) \end{bmatrix}. \tag{22}$$

In this equation, the partial derivatives of the surface on the left hand side represent the inline and crossline slopes of the surface, while $s_2(x, y, f^{i-1}(x, y))$ and $s_3(x, y, f^{i-1}(x, y))$ on the right hand side are the estimated seismic reflection slopes on the surface. This equation means that the slopes of the horizon surface should be approximately equal to the reflection slopes on the surface because a horizon surface should follow the reflections. However, at the beginning we actually do not know the correct position of the horizon surface. Therefore, we need to begin with an initial surface $f^0(x, y)$ (e.g. a flat surface $f^0(x, y) = z_0$), and then iteratively update the surface by solving the above equation until the surface slopes fit the reflection slopes at the i −th iteration (Wu & Hale 2015b).

Fig. 13(a) shows some horizons that are extracted by using the conventional slopes (Figs 11a and 12a). These extracted horizons can accurately follow the seismic reflections outside the carbonates but fail to follow the steep reflections inside the carbonates. Fig. 13(b) shows the horizons that are extracted by using the new

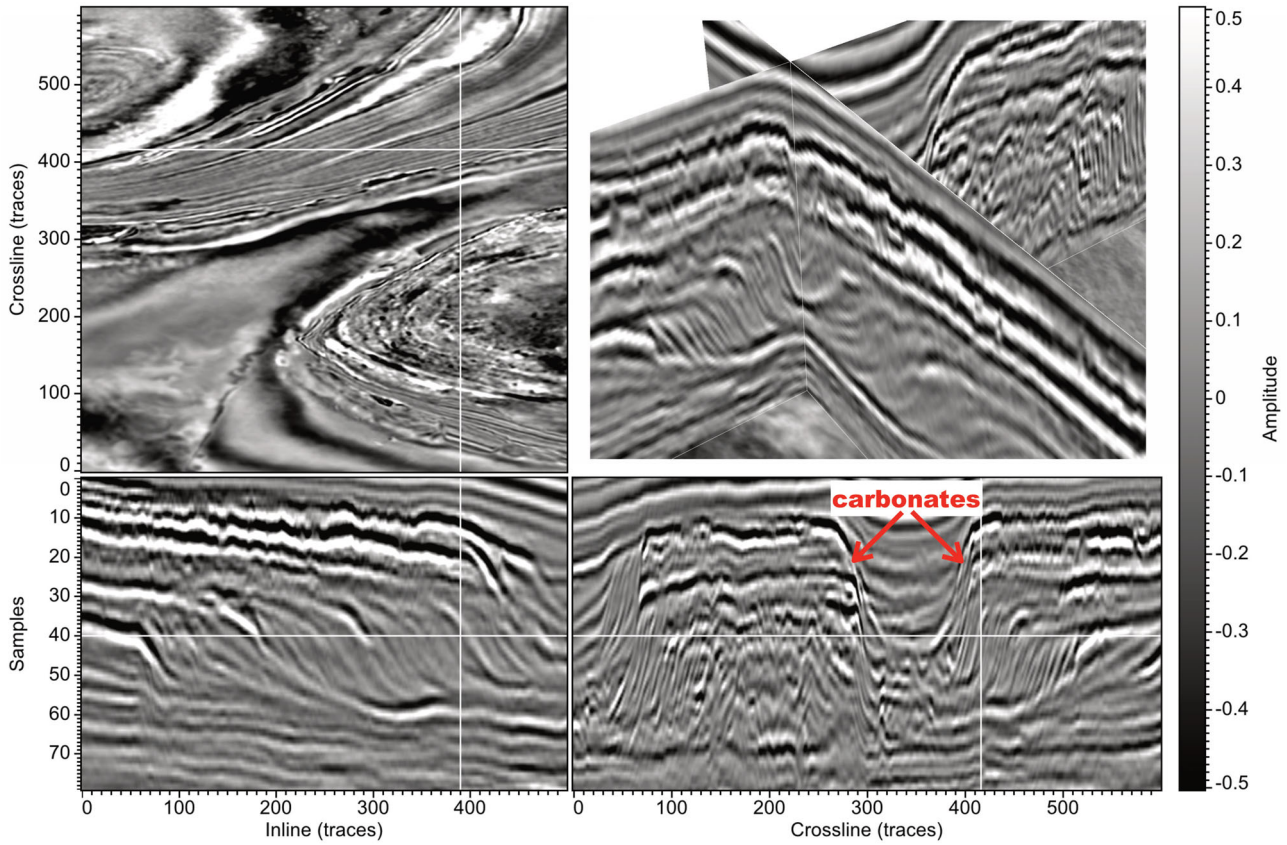

Figure 10. Three orthogonal slices of a 3-D seismic image and a 3D view (upper-right panel) of the image.

slopes (Figs 11b and 12b). We observe that these horizons better follow the steep and locally varying reflections than those (Fig. 13a) computed with conventional slopes. In extracting these horizons in Figs 13(a) and (b), we use exactly the same parameters for the horizon extraction method, and the only difference is the input slopes. This indicates that the new slopes (Figs 11b and 12b) computed from the directional structure tensors should be closer to the true reflection slopes than the slopes (Figs 11a and 12a) computed from the conventional structure tensors.

4.2 Stratigraphic orientations

To demonstrate how the directional structure tensors can better estimate stratigraphic orientations than the conventional structure tensors, we use another real 3-D seismic image with many channel features as shown on the horizon surface in Fig. 14. Fig. 15(a) shows a closer view of the seismic image in the dashed red box in Fig. 14.

In this example, we first construct conventional structure tensors (eq. 5) at all image samples and compute corresponding eigenvectors $\mathbf{w}$, which are supposed to be locally parallel to seismic stratigraphic features. In such a real seismic image, we do not know the true orientation of the stratigraphic features, and therefore it is difficult to quantitatively evaluate the errors in the estimated vectors $\mathbf{w}$. However, we can display the estimated vectors $\mathbf{w}$ as segments in the same 3-D view of the seismic image to visually evaluate if these segments are locally parallel to the stratigraphic features or not. In Fig. 15(a), we display the estimated vectors $\mathbf{w}$ as red segments at the samples on the extracted horizon surface. We observe that these segments are generally consistent with the obvious channels but are noisy and do not correctly follow the channels with relatively weaker features.

The red segments in Fig. 15(c) represent the vectors $\tilde{\mathbf{w}}$ computed from the 2-D directional structure tensors in eq. (16). In computing $\tilde{\mathbf{w}}$, we first use 3-D directional structure tensors (eq. 11) to estimate vectors $\tilde{\mathbf{u}}$ that are perpendicular to seismic reflections. From the estimated $\tilde{\mathbf{u}}$, we then compute orthogonal vectors $\tilde{\mathbf{p}}$ and $\tilde{\mathbf{q}}$ that are parallel to seismic reflections. With these vectors $\tilde{\mathbf{p}}$ and $\tilde{\mathbf{q}}$, we then construct the 2-D directional structure tensors (eq. 16) and compute the corresponding 2-D eigenvectors $\tilde{\mathbf{b}}$ (corresponding to the minimum eigenvalues) of the 2-D tensors. We finally compute the vectors $\tilde{\mathbf{w}}$ from $\tilde{\mathbf{u}}$ and $\tilde{\mathbf{b}}$ as shown in eq. (20). The normalized vectors $\tilde{\mathbf{w}}$, represented by red segments in Fig. 15(c), are locally much more consistent with the seismic channel features than the vectors $\mathbf{w}$ represented by red segments in Fig. 15(b). This indicates that the vectors $\tilde{\mathbf{w}}$, computed from the proposed directional structure tensors, provide a better estimation of the stratigraphic orientations than the vectors $\mathbf{w}$ computed from the conventional structure tensors.

5 CONCLUSIONS

Conventional structure tensors can be used to accurately estimate orientations of reflections with slightly dipping and slowly varying slopes, but often yield errors in estimating orientations of the structures with steep and rapidly varying slopes. Therefore, we propose a method to estimate reflection orientations in a new space, where the reflections are almost flat or slightly dipping and the slope variations are decreased. In this method, we do not transform the seismic image into the new space, instead, we compute local derivatives in

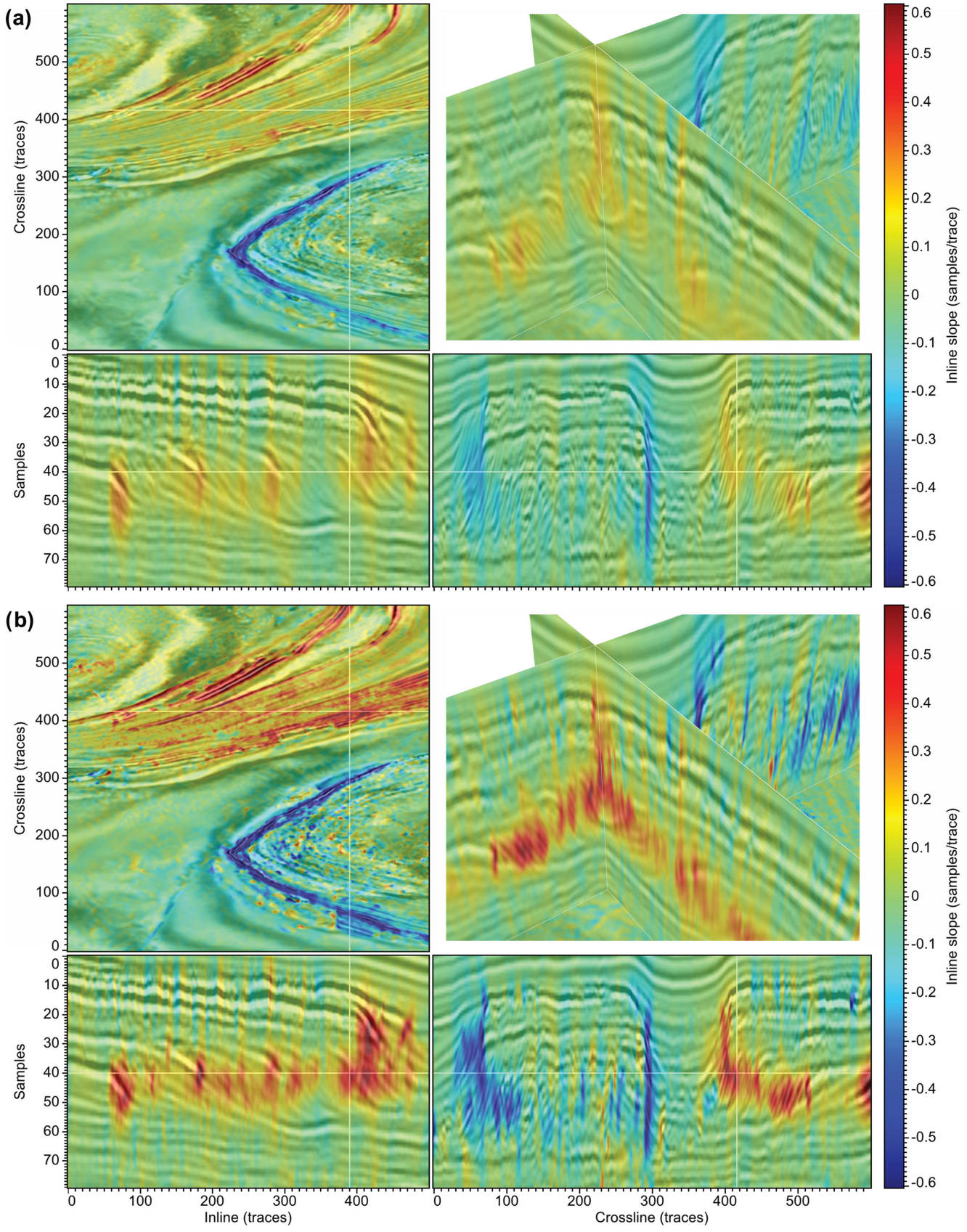

Figure 11. Inline slopes are estimated using conventional (a) and directional (b) structure tensors.

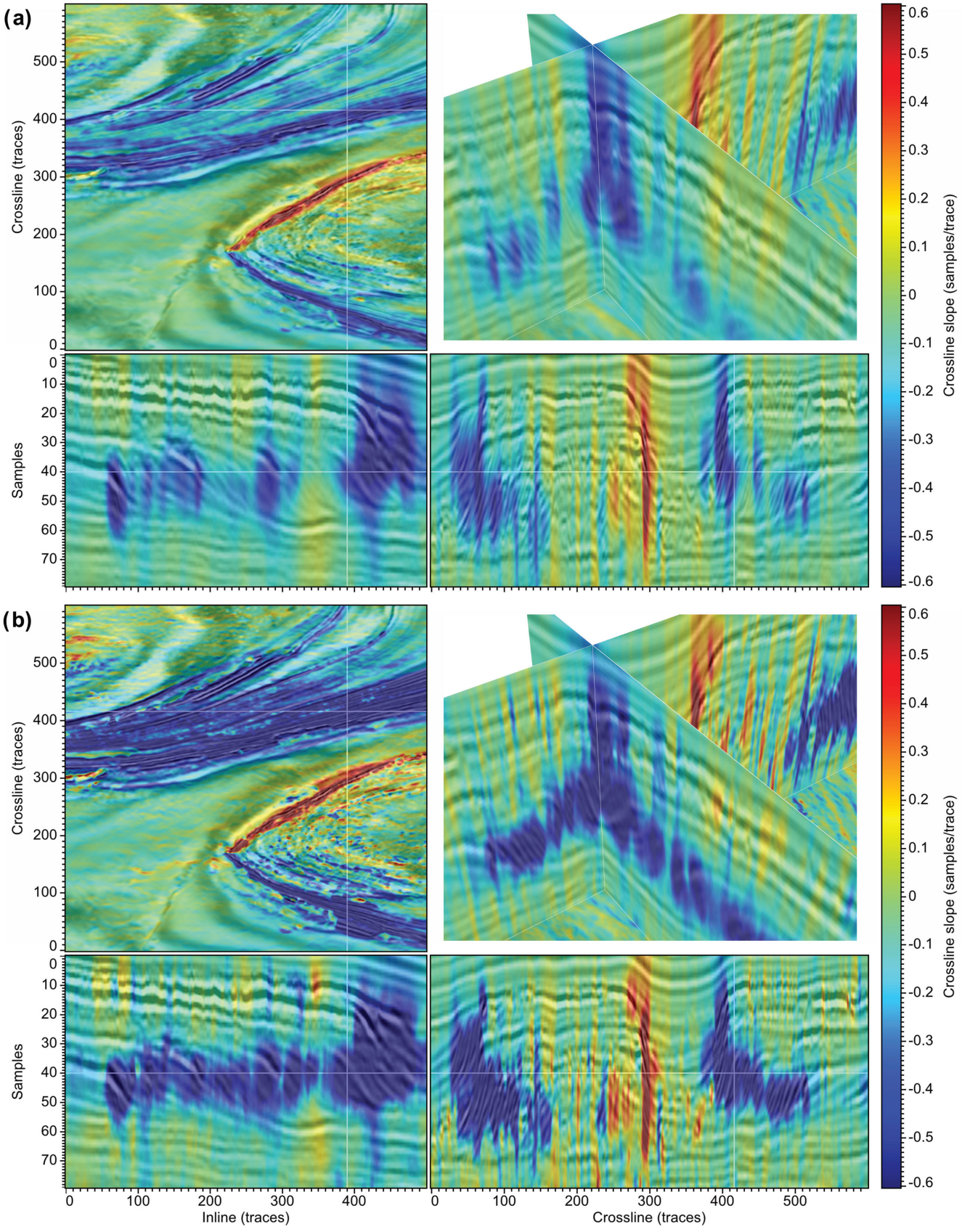

Figure 12. Crossline slopes are estimated using conventional (a) and directional (b) structure tensors.

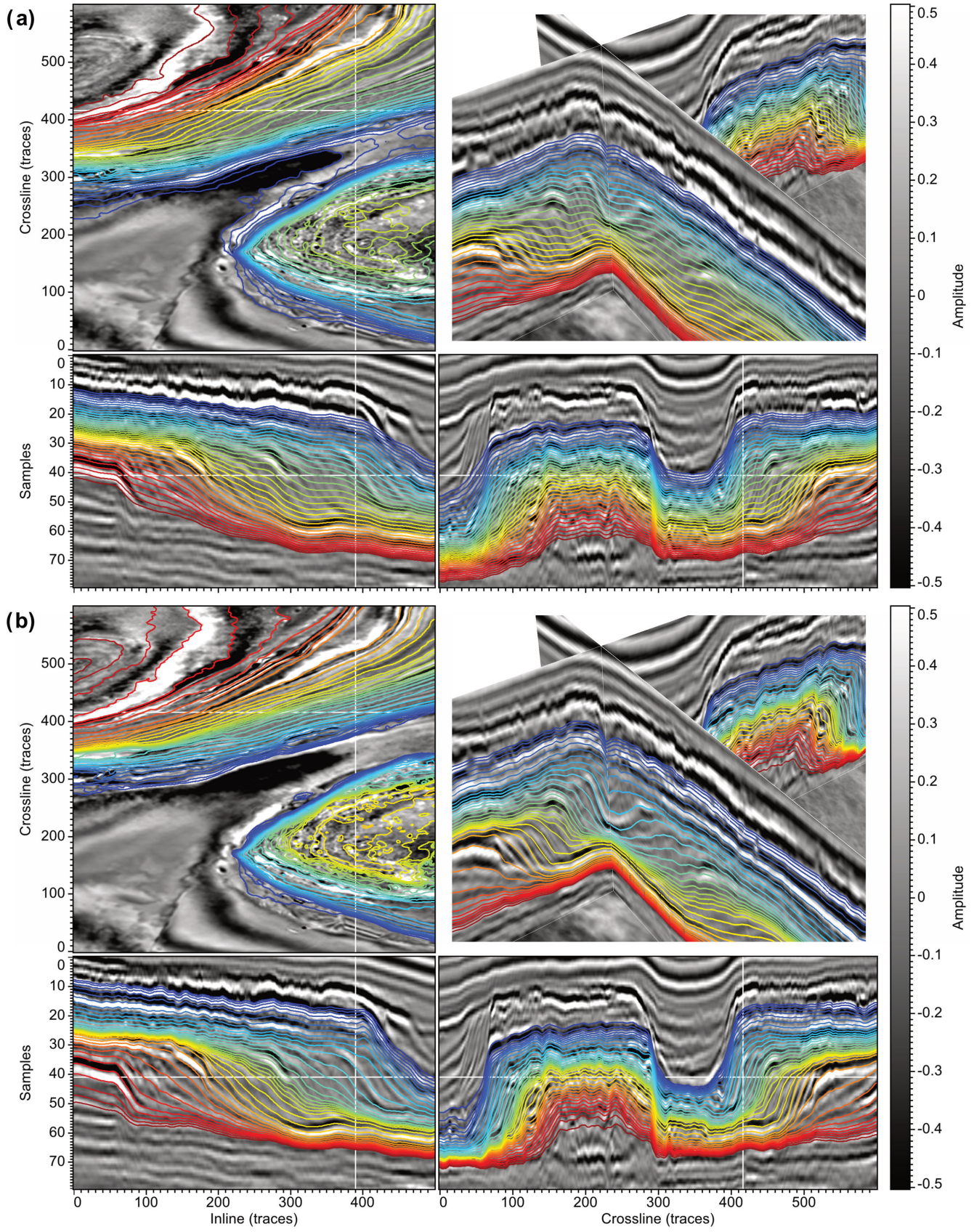

Figure 13. Horizons displayed in (a) and (b) are extracted using conventional (Figs 11 a and 12a) and improved (Figs 11 b and 12b) slopes, respectively.

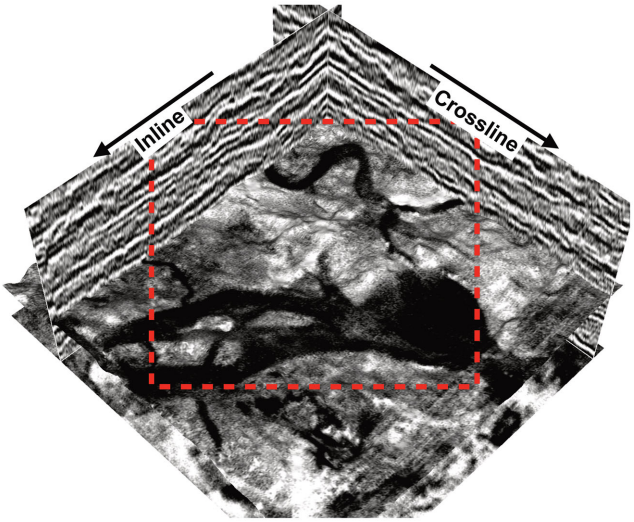

Figure 14. A 3-D seismic image is displayed a horizon surface, which is extracted from the seismic image by following seismic reflections. Black channel features are apparent on the horizon surface.

that space and use these derivatives to construct structure tensors in the new space. From the directional structure tensors, we estimate the normal vectors of the flat or slightly dipping reflections in the new space and then transform the vectors back to obtain a better estimation of reflection normals in the original space. The computational cost of our directional structure-tensor method in estimating reflection normals is about two times of the conventional method because the our method requires first computing an initial estimation of reflection normals.

To estimate stratigraphic orientations in 3-D cases, we first estimate the lateral orientations of the stratigraphic features using 2-D directional structure tensors constructed with directional derivatives computed along seismic reflections. This is equivalent to first extract a horizon surface following reflections, and then construct structure tensors with gradients along the surface to estimate the lateral orientations of stratigraphic features apparent on the surface. We then compute the 3-D orientations of the stratigraphic features by combining the lateral orientations with the estimated reflections normals.

One limitation of our methods exists in estimating discontinuous structural and stratigraphic orientations in areas where the reflections and channels are dislocated by faults or terminated by unconformities. This is also a common limitation for the conventional structure-tensor method and other methods. Our methods might be further improved by using spatially variant smoothing in constructing the directional structure tensors, so that the smoothing is stopped or the smoothing extents are reduced near the faults or unconformities.

ACKNOWLEDGEMENTS

The Poseidon 3-D seismic volume was acquired through the public release of data of Geoscience Australia. The seismic image of buried channels is a subset of the Parihaka 3-D data set provided by New Zealand Crown Minerals through the SEG Wiki website (http://wiki.seg.org/wiki/Parihaka-3D). This research is supported by the sponsors of the Texas Consortium for Computational Seismology (TCCS).

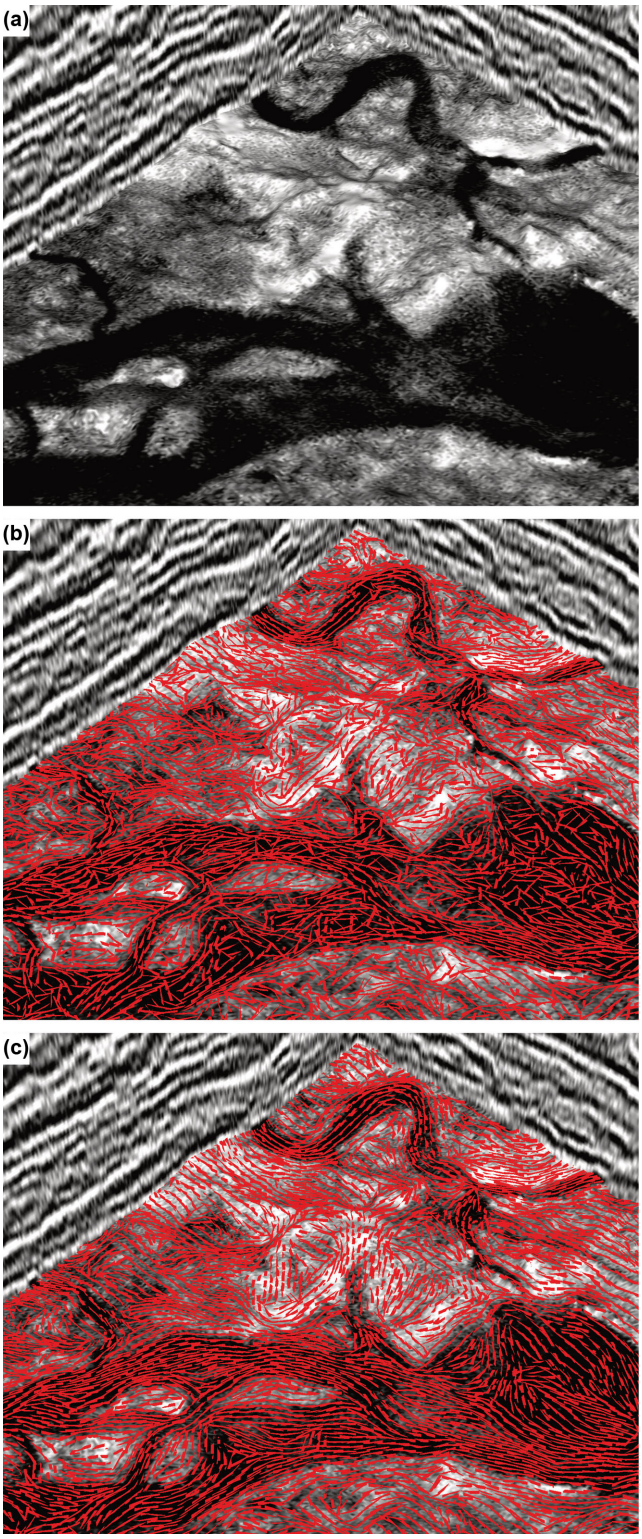

Figure 15. (a) A closer view of the seismic image in the dashed red box in Fig. 14. The red segments in (b) and (c) represent the 3-D vectors $\mathbf{w}$ and $\tilde{\mathbf{w}}$ computed from the conventional (eq. 5) and directional (eq. 16) structure tensors, respectively.

REFERENCES

Arias, E., 2016. Estimating seismic reflection slopes, *Master's thesis,* Colorado School of Mines.

Bakker, P., 2002. Image structure analysis for seismic interpretation, *PhD thesis,* Delft University of Technology.

Claerbout, J.F., 1992. *Earth Soundings Analysis: Processing Versus Inversion,* Blackwell Science.

Clapp, R.G., Biondi, B.L. & Claerbout, J.F., 2004. Incorporating geologic information into reflection tomography, *Geophysics,* **69**(2), 533–546.

de Groot, P., de Bruin, G. & Hemstra, N., 2006. How to create and use 3d wheeler transformed seismic volumes, in *76th Annual International Meeting, SEG, Expanded Abstracts,* pp. 1038–1042.

Di, H. & Gao, D., 2016. Improved estimates of seismic curvature and flexure based on 3D surface rotation in the presence of structure dip, *Geophysics,* **81**(2), IM13–IM23.

Fehmers, G.C. & Höcker, C.F., 2003. Fast structural interpretation with structure-oriented filtering, *Geophysics,* **68**(4), 1286–1293.

Field, D.J., 1987. Relations between the statistics of natural images and the response properties of cortical cells, *J. Opt. Soc. Am. A,* **4**(12), 2379–2394.

Fomel, S., 2002. Applications of plane-wave destruction filters, *Geophysics,* **67**(6), 1946–1960.

Fomel, S., 2010. Predictive painting of 3D seismic volumes, *Geophysics,* **75**(4), A25–A30.

Hale, D., 2009a. Image-guided blended neighbor interpolation of scattered data, in *79th Annual International Meeting, SEG, Expanded Abstracts,* pp. 1127–1131.

Hale, D., 2009b. Structure-oriented smoothing and semblance, CWP Report 635.

Hale, D., 2013. Dynamic warping of seismic images, *Geophysics,* **78,** S105–S115.

Howarth, V. & Alves, T.M., 2016. Fluid flow through carbonate platforms as evidence for deep-seated reservoirs in northwest Australia, *Mar. Geol.,* **380,** 17–43.

Karimi, P. & Fomel, S., 2015. Stratigraphic coordinates: a coordinate system tailored to seismic interpretation, *Geophys. Prospect.,* **63**(5), 1246–1255.

Köthe, U., 2003. Edge and junction detection with an improved structure tensor, in *Joint Pattern Recognition Symposium,* pp. 25–32, eds Michaelis, B. & Krell, G., Springer.

Li, Y. & Oldenburg, D.W., 2000. Incorporating geological dip information into geophysical inversions, *Geophysics,* **65**(1), 148–157.

Lomask, J., Guitton, A., Fomel, S., Claerbout, J. & Valenciano, A.A., 2006. Flattening without picking, *Geophysics,* **71**(4), 13–20.

Luo, S. & Hale, D., 2013. Unfaulting and unfolding 3D seismic images, *Geophysics,* **78**(4), O45–O56.

Ma, Y., Hale, D., Gong, B. & Meng, Z.J., 2012. Image-guided sparse-model full waveform inversion, *Geophysics,* **77**(4), R189–R198.

Mallet, J., 2014. *Elements of Mathematical Sedimentary Geology: The GeoChron Model,* EAGE Publications.

Mallet, J.-L., 2004. Space-time mathematical framework for sedimentary geology, *Math. Geol.,* **36**(1), 1–32.

Mallet, J.-L.L., 2002. *Geomodeling,* Oxford Univ. Press, Inc.

Marfurt, K.J., 2006. Robust estimates of 3D reflector dip and azimuth, *Geophysics,* **71**(4), P29–P40.

Parks, D., 2010. Seismic image flattening as a linear inverse problem, *Master's thesis,* Colorado School of Mines.

van de Weijer, J., 2005. Color features and local structure in images, *PhD thesis,* Univ. Amsterdam.

Van Vliet, L.J. & Verbeek, P.W., 1995. Estimators for orientation and anisotropy in digitized images, in *Proceedings of the First Annual Conference of the Advanced School for Computing and Imaging ASCI'95,* Heijen, The Netherlands, pp. 442–450.

Weickert, J., 1997. A review of nonlinear diffusion filtering, in *Scale-Space Theory in Computer Vision,* vol. 1252 of Lecture Notes in Computer Science, pp. 1–28, eds ter Haar Romeny, B., Florack, L., Koenderink, J. & Viergever, M., Springer.

Weickert, J., 1999. Coherence-enhancing diffusion filtering, *Int. J. Comput. Vis.,* **31**(2-3), 111–127.

Wu, X., 2017a. Building 3D subsurface models conforming to seismic structural and stratigraphic features, *Geophysics,* **82**(3), IM21–IM30.

Wu, X., 2017b. Structure-, stratigraphy-, and fault-guided regularization in geophysical inversion, *Geophys. J. Int.,* **210**(1), 184–195.

Wu, X. & Hale, D., 2013. Extracting horizons and sequence boundaries from 3D seismic images, in *83rd Annual International Meeting, SEG, Expanded Abstracts,* pp. 1440–1445, Soc. of Expl. Geophys.

Wu, X. & Hale, D., 2015a. 3D seismic image processing for unconformities, *Geophysics,* **80**(2), IM35–IM44.

Wu, X. & Hale, D., 2015b. Horizon volumes with interpreted constraints, *Geophysics,* **80**(2), IM21–IM33.

Yu, Y., Kelley, C. & Mardanova, I., 2013. Volumetric seismic dip and azimuth estimation with 2D Log-Gabor filter array, in *83rd Annual International Meeting, SEG, Expanded Abstracts,* pp. 1357–1362.